Poly-*N*-Acetylglucosamine Production by *Staphylococcus epidermidis* Cells Increases Their *In Vivo* Proinflammatory Effect

Pedro Ferreirinha,[a,b,c] Begoña Pérez-Cabezas,[a,b] Alexandra Correia,[a,b] Bruna Miyazawa,[d] Angela França,[e] Virgínia Carvalhais,[e] Augusto Faustino,[c] Anabela Cordeiro-da-Silva,[a,b,f] Luzia Teixeira,[c,g] Gerald B. Pier,[h] Nuno Cerca,[e] Manuel Vilanova[a,b,c]

Instituto de Investigação e Inovação em Saúde[a] and IBMC, Instituto de Biologia Molecular e Celular,[b] Universidade do Porto, Porto, Portugal; ICBAS-UP, Instituto de Ciências Biomédicas de Abel Salazar, Universidade do Porto, Porto, Portugal[c]; Unidade de Pesquisa Clínica do Hospital das Clínicas da Faculdade de Medicina de Ribeirão Preto da Universidade de São Paulo (UPC-HCFMRP-USP), São Paulo, Brazil[d]; CEB-LIBRO, Centro de Engenharia Biológica, Laboratório de Investigação em Biofilmes Rosário Oliveira, University of Minho, Campus de Gualtar, Braga, Portugal[e]; Department of Biological Sciences, Faculty of Pharmacy, University of Porto, Porto, Portugal[f]; UMIB, Unidade Multidisciplinar de Investigação Biomédica, Universidade do Porto, Porto, Portugal[g]; Division of Infectious Diseases, Department of Medicine, Brigham and Women's Hospital/Harvard Medical School, Boston, Massachusetts, USA[h]

Poly-*N*-acetylglucosamine (PNAG) is a major component of the *Staphylococcus epidermidis* biofilm extracellular matrix. However, it is not yet clear how this polysaccharide impacts the host immune response and infection-associated pathology. Faster neutrophil recruitment and bacterial clearance were observed in mice challenged intraperitoneally with *S. epidermidis* biofilm cells of the PNAG-producing 9142 strain than in mice similarly challenged with the isogenic PNAG-defective M10 mutant. Moreover, intraperitoneal priming with 9142 cells exacerbated liver inflammatory pathology induced by a subsequent intravenous *S. epidermidis* challenge, compared to priming with M10 cells. The 9142-primed mice had elevated splenic CD4$^+$ T cells producing gamma interferon and interleukin-17A, indicating that PNAG promoted cell-mediated immunity. Curiously, despite having more marked liver tissue pathology, 9142-primed mice also had splenic T regulatory cells with greater suppressive activity than those of their M10-primed counterparts. By showing that PNAG production by *S. epidermidis* biofilm cells exacerbates host inflammatory pathology, these results together suggest that this polysaccharide contributes to the clinical features associated with biofilm-derived infections.

*S*taphylococcus epidermidis is a commensal bacterium of human skin and mucous membranes (1). The ability to establish biofilms on the surfaces of indwelling medical devices is a major virulence mechanism of this bacterium, which is the most commonly isolated etiological agent of nosocomial infections (2). *S. epidermidis* biofilm formation involves initial cellular adherence to a surface, followed by intercellular aggregation and accumulation in multilayer cell clusters (1). This process is dependent on adhesive extracellular molecules (3) such as poly-*N*-acetylglucosamine (PNAG). PNAG is a major factor mediating cell-to-cell adhesion in staphylococci (4, 5), and its production depends on genes encoded within the intercellular adhesion (*ica*) locus (6). The final stage of the biofilm life cycle comprises cell disassembly and subsequent growth in a planktonic mode, a process contributing to *S. epidermidis* biofilm pathogenesis by disseminating infection (7).

S. epidermidis strains with impaired PNAG production display attenuated virulence in foreign body infection models (8, 9), while the production of this polysaccharide conferred a survival advantage on this bacterium infecting the nematode host *Caenorhabditis elegans* (10). Moreover, *ica* mutants display growth attenuation when competing *in vivo* with the corresponding wild-type (WT) strains (11) and commensal *ica*-negative strains became invasive when transformed with a plasmid containing the *ica* locus (12). In the clinical setting, the presence of *icaA/D* genes was associated with therapeutic failure in device-related infections with coagulase-negative staphylococci (13). Despite the observed association of PNAG production with *S. epidermidis* virulence, it is not entirely clear how this polysaccharide may affect the host immune response. Previous reports have shown that PNAG stimulates the production of proinflammatory mediators (14, 15) but also that it impairs phagocytosis and phagocyte-mediated bacterial killing

(16–18). Additionally, little is known about the effects of this polysaccharide on acquired immunity. Here, by using the PNAG-producing *S. epidermidis* 9142 strain and a PNAG-negative isogenic M10 mutant, we have addressed in the murine model how this polysaccharide affected the host inflammatory response. The results obtained show that mice infected with a PNAG-producing *S. epidermidis* strain exhibited a more intense inflammatory response than mice infected with an isogenic PNAG-negative mutant.

MATERIALS AND METHODS

Bacteria and growth conditions. Biofilm-forming *S. epidermidis* strain 9142 (19) and the isogenic PNAG-negative M10 mutant (5) were used. Absence of growth defects in the M10 strain was confirmed, as the two strains had similar generation times, as determined by growing 9142 and M10 bacteria in tryptic soy broth (TSB; Merck, Darmstadt, Germany).

Abrogation of PNAG production in M10 cells was confirmed by flow cytometry (see Fig. S1 in the supplemental material). To prepare bacterial suspensions for inoculation, both strains were grown simultaneously for 48 h in TSB under biofilm-inducing conditions as previously described (20). Additionally, 48-h 9142 biofilm culture supernatants were recovered to collect biofilm-released cells (21), designated S-9142 cells here. For details of the methods used, see Fig. S2 in the supplemental material. Bacterial suspensions were mildly sonicated to dissociate cell clusters and create a homogeneous suspension. Cell concentrations and viability were determined by flow cytometry by previously described methods (20).

Mice. Male BALB/c mice 8 to 12 weeks old were purchased from Charles River and housed at the animal facilities of ICBAS-UP. Interleukin-10 (IL-10)-deficient ($Il10^{-/-}$) BALB/c mice 8 to 12 weeks old were kindly provided by Anne O'Garra (National Institute for Medical Research, London, United Kingdom) and housed at the animal facilities of IBMC. Procedures were performed according to the 86/609/EEC Directive and Portuguese rules (DL 129/92) and were approved by the competent national board (DGV, document 0420/000/000/2010).

Infections and collection of biological samples. For analysis of early inflammatory responses, mice were infected intraperitoneally (i.p.) with 2×10^8 live 9142 or M10 cells or sham infected with phosphate-buffered saline (PBS). Animals were anesthetized with isoflurane (Abbott House, Berkshire, United Kingdom) for terminal blood collection and euthanasia. Peritoneal exudates were recovered in 5 ml of cold PBS. Exudates contaminated with blood were excluded. Collected cells were used for flow cytometry analysis. Livers were collected in PBS, disrupted with a Potter homogenizer, serially diluted, and plated on tryptic soy agar (Merck) for enumeration of CFU. To analyze the induction of acquired immunity, BALB/c mice were primed twice i.p. at 1-week intervals with 1×10^6 live 9142 or M10 cells or PBS alone. Control groups were not subjected to further treatment (9142/−, M10/−, or PBS/− mice, respectively). Seven days after the last i.p. immunization, mice from all groups were also intravenously (i.v.) challenged with 1×10^8 CFU of S-9142 bacteria (9142/S-9142, M10/S-9142, and PBS/S-9142 mice). Four and 9 days after infection, animals were anesthetized for blood collection and euthanized as described above. Spleens were removed and homogenized to single-cell suspensions in Hanks' balanced salt solution (Sigma) for further use in flow cytometry and *in vitro* suppression assays. Livers were also collected and used for CFU counting or histopathologic analysis. $Il10^{-/-}$ mice were similarly tested but challenged i.v. with 1×10^7 S-9142 bacteria. Experimental mouse groups are schematically described in Fig. S2 in the supplemental material.

Flow cytometry analysis. Flow cytometry analysis was performed with an EPICS XL flow cytometer with the EXPO32ADC software (Beckman Coulter, Miami, FL). A subset of a total of 1×10^6 leukocytes was stained per sample. The following anti-mouse monoclonal antibodies (MAbs), along with the respective isotype controls, were used: F4/80 antigen (BM8), Foxp3 (FJK-16S) (both from eBioscience, San Diego, CA), CD4 (RM4-5), Ly-6G (1A8), Ly-6C (AL-21), CD25 (PC61), gamma interferon (IFN-γ) (XMG1.2), IL-4 (BVD4-11B11), IL-17A (TC11-18H10), and IL-10 (JES5-2A5) (all from BD Pharmingen, San Diego, CA, USA). For intracellular cytokine detection, cells were stimulated with phorbol myristate acetate and ionomycin in the presence of brefeldin A as previously described (22). Detection of surface cell markers and intracellular Foxp3 was performed also as previously described (22). The collected data files were analyzed with FlowJo software version vX.0.7 (Tree Star Inc., Ashland, OR, USA).

Cytokine measurements. The concentrations of CXCL-1, CXCL-2, tumor necrosis factor alpha (TNF-α), IL-6, IL-10, IL-12p70, IFN-γ, and IL-17A in peritoneal exudates or serum samples were evaluated with commercial enzyme-linked immunosorbent assay (ELISA) kits (Duo-Set; R&D Systems, Minneapolis, MN, USA).

Antibody titer quantification. *S. epidermidis*-specific serum IgG antibody titers were quantified by ELISA and calculated by endpoint titration of serial dilutions. ELISA plates (MaxiSorp; Nunc, Roskilde, Denmark) were coated with isopropanol-fixed S-9142 cells at 1×10^6/well. Bound serum antibodies were detected with alkaline phosphatase-coupled goat anti-mouse anti-IgG1, -IgG2a, or -IgG3 (Southern Biotechnology Associates, Birmingham, AL, USA).

IFN-γ neutralization. To neutralize IFN-γ, mice were i.v. injected in the tail vein 1 h prior to infection (performed as described above) with 500 μg of an IFN-γ-specific MAb (clone R4-6A2) or a rat IgG1 isotype control (clone HRPM), both from BioXcell, West Lebanon, NH, USA.

Cell cultures and suppression assays. *In vitro* suppression assays were performed according to a modification of previously described methods (22). Briefly, antigen-presenting cells (APC) were prepared from splenic cell suspensions of naive mice. Total CD4$^+$, CD4$^+$ CD25$^-$, and CD4$^+$ CD25$^+$ cells from noninfected and infected mice were isolated from pooled spleen cells of five mice with a magnetic cell sorting CD4$^+$ CD25$^+$ T-cell isolation kit (Miltenyi Biotech, Inc., Auburn, CA, USA). Naive, carboxyfluorescein succinimidyl ester (CFSE)-labeled, CD4$^+$ CD25$^-$ T cells (responder cells) were plated at 2.5×10^4/well into U-shaped 96-well plates together with 10^5 APC and 1 μg/ml anti-CD3 MAb (positive controls). Cells without the anti-CD3 stimulus were used as negative controls. CD4$^+$ CD25$^+$ T cells from the different groups analyzed were added at different CD4$^+$ CD25$^+$-to-responder T-cell ratios (1:1, 0.5:1, 0.2:1, and 0.1:1). Each condition was set in sextuplicate, and cultures were maintained for 72 h at 37°C and 5% CO$_2$. Proliferation and suppression were determined on the basis of CFSE fluorescence by flow cytometric analysis in an EPICS XL flow cytometer (Beckman-Coulter).

Histopathologic examination and immunohistochemistry. Livers were fixed in buffered formalin and embedded in paraffin for hematoxylin-eosin (HE) histopathologic analysis or Foxp3 detection by immunohistochemistry as previously described (23). For histopathologic analysis of WT and $Il10^{-/-}$ mice, five micrographs at ×100 magnification, from five different liver lobes, were randomly taken from each tissue slide sample. The number of cellular infiltrate clusters was determined with ImageJ software (National Institutes of Health, Bethesda, MD). For Foxp3 detection in either WT or $Il10^{-/-}$ mice, representative micrographs of each tissue slide sample were taken at ×400 magnification.

Statistical analysis. Statistical significance of results was determined by one-way analysis of variance (ANOVA) and Tukey's *post hoc* test. Statistical analysis was performed with GraphPad Prism 5 Software (GraphPad Software, Inc., La Jolla, CA, USA). P values of <0.05 were considered statistically significant.

RESULTS

Inflammatory response in mice infected with 9142 or M10 *S. epidermidis*. To assess the effect of PNAG production on the early inflammatory response to *S. epidermidis* infection, peritoneal exudates were recovered from mice 2 and 6 h after infection with 9142 or M10 or from PBS-treated controls. Higher levels of the neutrophil-chemokine attractant CXCL-1 were found in the exudates of infected mice than in those of controls (Fig. 1A). CXCL-2 levels were found transiently above control values in both infected mouse groups, albeit not reaching statistical significance. In accordance with these findings, neutrophils, defined as Ly6G^{high} Ly6C$^{low/int}$ F4/80$^{neg/low}$ cells (24), were rapidly recruited into the peritoneal cavities of all infected animals (Fig. 2A and B). Two hours after infection, higher numbers of recruited neutrophils were found in mice infected with 9142 than in M10-infected mice, while the reverse was observed by 6 h postinfection (Fig. 2B). The levels of the proinflammatory cytokines TNF-α, IL-6, and IL-12p70, as well as of antiinflammatory IL-10, were also assessed in the peritoneal lavage fluids. Both infected mouse groups showed elevated IL-6 levels, which were higher in 9142-infected mice (Fig. 1A). Serum IL-6 was also found to be elevated in both infected groups (Fig. 1B). The IL-10 concentration was found slightly
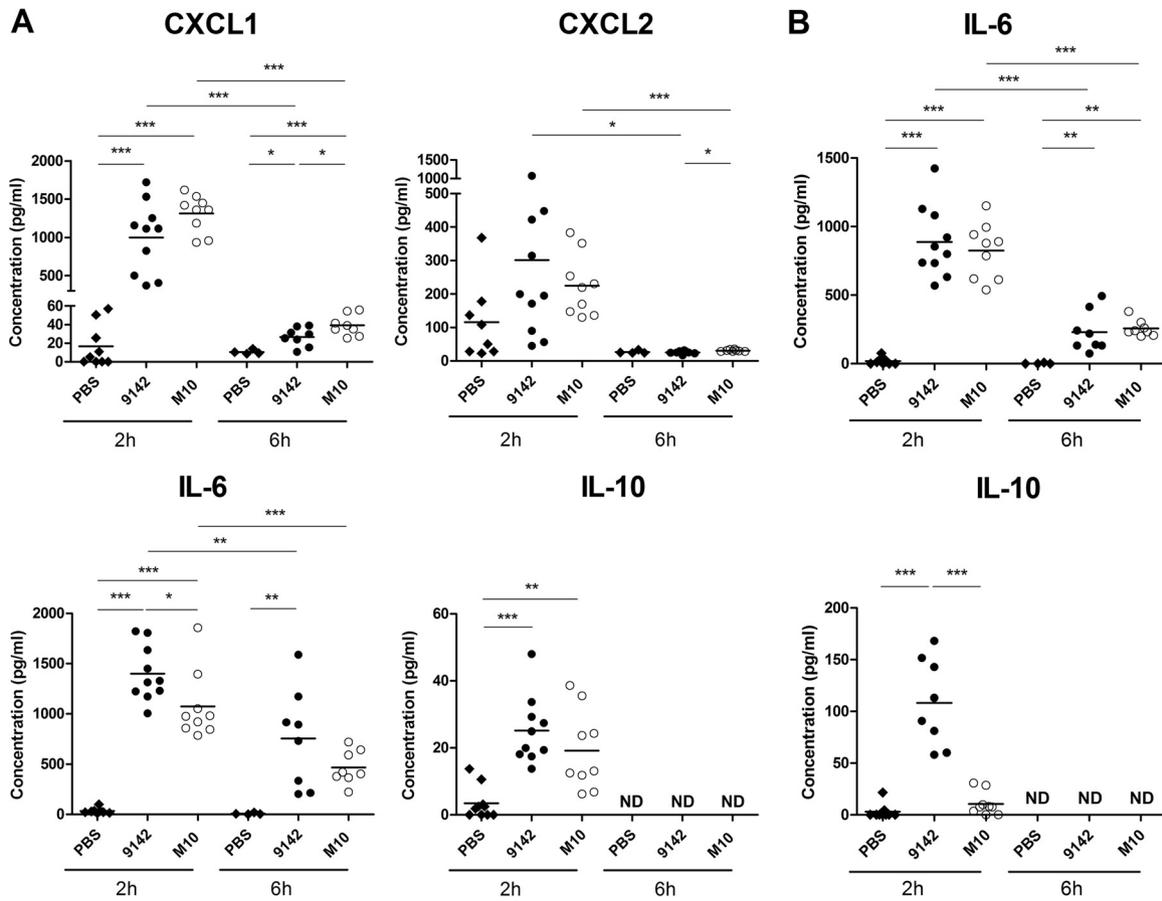
FIG 1 Cytokine production 2 and 6 h following i.p. infection with *S. epidermidis* cells. Levels of CXCL1, CXCL2, IL-6, and IL-10 (A), as indicated, in the peritoneal exudates and IL-6 and IL-10 (B) in the serum of *S. epidermidis* 9142-, M10-, or PBS-injected mice. Results correspond to pooled data of three independent experiments for each time point analyzed. Each dot represents an individual mouse. The horizontal line in each group represents the mean value; ND, not detected above the limit of detection. One-way ANOVA, $P < 0.05$, with Tukey's *post hoc* test: *, $P < 0.05$; **, $P < 0.01$; ***, $P < 0.001$.

above control levels in peritoneal exudates obtained from both infected groups at 2 h postinfection, while serum IL-10 was detected above control levels only in 9142-infected mice (Fig. 1A and B, respectively). No increase in TNF-α and IL-12p70 levels was detected in either the sera or peritoneal exudates (data not shown). As shown in Fig. 2C and D, the loads of the two bacterial strains in the peritoneal exudates and livers were similar at 2 h postinfection, but the elimination of strain 9142 was faster at 6 h than that of strain M10. *S. epidermidis* CFU were no longer detected in any group 24 h after infection. These results together show that PNAG expression promotes faster recruitment of neutrophils and improved bacterial clearance.

Acquired immune response in mice primed with 9142 or M10 *S. epidermidis*. We next used a prime-boost strategy with PNAG-producing or -nonproducing bacteria to assess how this polysaccharide affected the adaptive immune response to *S. epidermidis* infection. Since biofilm-derived cells can disseminate hematogenously (25), we used an i.v. challenge model. BALB/c mice were primed with *S. epidermidis* 9142 or M10 cells grown under biofilm-inducing conditions and challenged i.v. with S-9142 cells. Unexpectedly, prior immunization with either strain made mice more susceptible to an i.v. challenge, preventing prompt elimination of the pathogen (see Table S1 in the supplemental material). To understand the basis of this phenomenon, we analyzed a series

of immune parameters. Prior immunization with either strain increased the *S. epidermidis*-specific IgG titers (Fig. 3), suggesting that there was no impairment of antibody responses. We found evidence of an enhanced T-cell response in mice immunized with strain 9142. As shown in Fig. 4, these mice presented higher proportions and numbers of splenic IFN-γ$^+$ CD4$^+$ and IL-17A$^+$ CD4$^+$ T cells than mice primed with M10 or the PBS-treated controls. No increase in IL-4- or IL-10-expressing CD4$^+$ T cells appeared to be promoted by immunization. No significant elevation of serum IFN-γ or IL17A was found in immunized mice compared to the control group (see Fig. S3 in the supplemental material).

Effect of PNAG production on liver inflammatory pathology. Liver histopathology was analyzed in the infected mice, as this organ is a preferred target in i.v. *S. epidermidis* infection (26). No bacteria could be found in the nonchallenged control groups, and their livers presented no significant histological alterations (see Fig. S4 in the supplemental material). Challenged mice showed liver lesions that were more numerous and occupied a larger area in mice previously immunized by either strain than in PBS-treated controls. Immunization with strain 9142 led to a more intense inflammatory response than immunization with strain M10 (Fig. 5A and B). Mice from the former group showed well-defined granulomas, and rare plasma cells were also observed (see Fig. S5
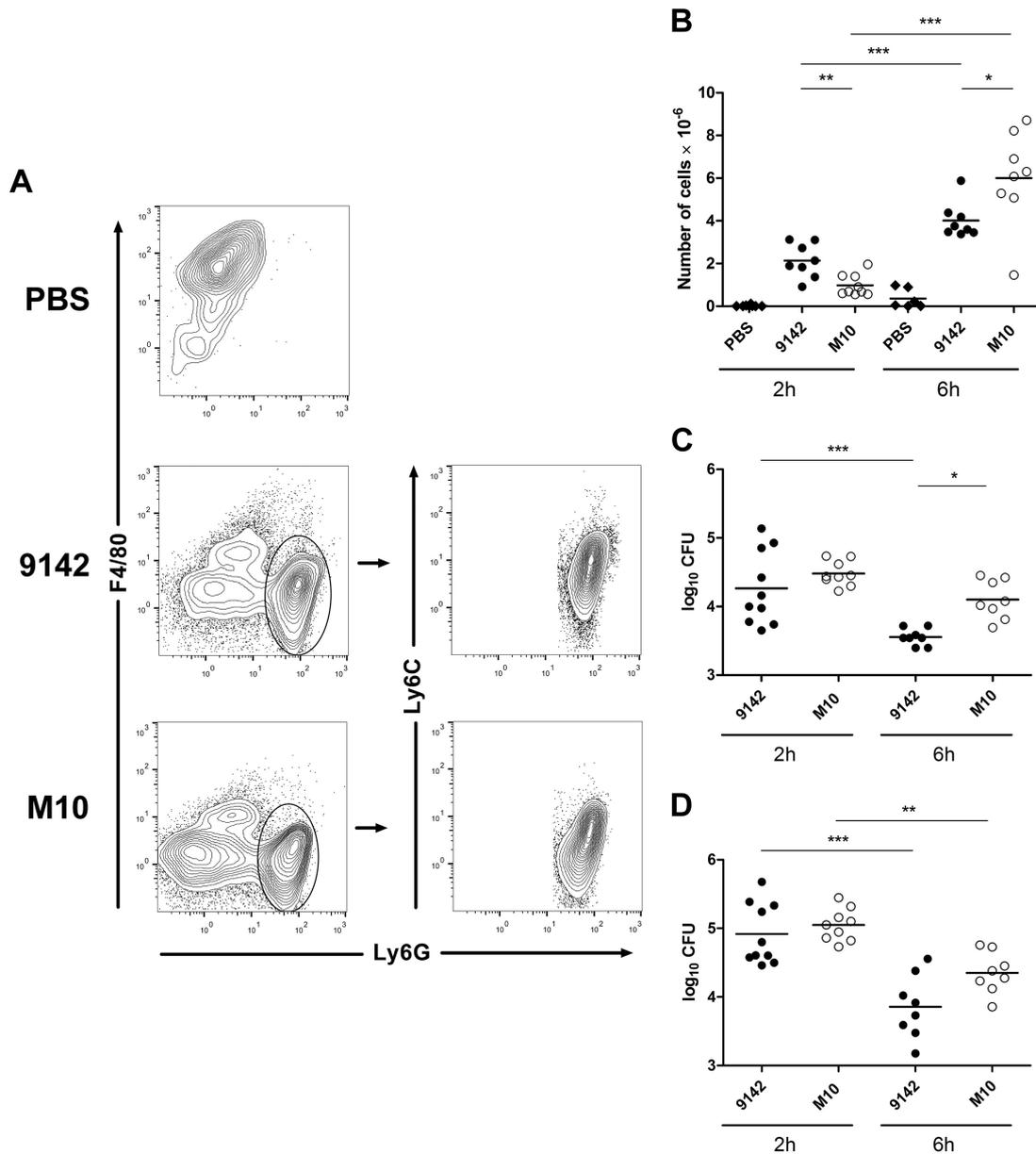
FIG 2 Neutrophil and CFU counts of *S. epidermidis* in the peritoneal cavity 2 and 6 h after infection. (A, B) Contour plots representative of the gating strategy used to define neutrophils (Ly6G^{high} Ly6C$^{low/int}$ F4/80$^{neg/low}$) (A) and numbers of neutrophils in the peritoneal exudates of *S. epidermidis* 9142-, M10-, or PBS-injected mouse groups (B). One-way ANOVA, $P < 0.05$, with Tukey's *post hoc* test: *, $P < 0.05$; **, $P < 0.01$; ***, $P < 0.001$. (C, D) Numbers of CFU recovered at the indicated time points after infection from the peritoneal exudates (C) and livers (D) of the same mouse groups. Results correspond to pooled data of three independent experiments for each time point analyzed. Each dot represents an individual mouse. The horizontal line in each group represents the mean value. One-way ANOVA, $P < 0.05$, with Tukey's *post hoc* test: *, $P < 0.05$; **, $P < 0.01$; ***, $P < 0.001$.

in the supplemental material). The presence of polymorphonuclear cells (two or three per high-power magnification field) was also observed (Fig. 5C). In mice immunized with M10, the infiltration remained mostly lymphocytic. Mitotic hepatocytes and large necrotic areas were observed in two animals immunized with strain 9142, both at the periphery and in the parenchyma of the tissue (Fig. 5C). At day 9 after the i.v. challenge, 9142/S-9142 mice still presented the more marked inflammatory response (see Fig. S6 in the supplemental material). Together, these findings confirmed the proinflammatory effect of bacterial PNAG production. As IFN-γ has been associated with the formation of granulomas

(27), we next evaluated the effect of neutralizing this cytokine in the i.v. infected mice. Surprisingly, as shown in Fig. S7 in the supplemental material, bacterium-primed mice treated with a neutralizing anti-IFN-γ MAb before the i.v. challenge presented higher numbers of liver infiltrates than isotype control-treated counterparts. This result indicates a rather protective role for IFN-γ in the observed liver histopathology.

Suppressive activity of regulatory T cells in *S. epidermidis*-infected mice. We next investigated whether the proinflammatory role of PNAG could result from impaired regulatory T-cell (Treg cell) responses or function. As shown in Fig. S7 in the sup-
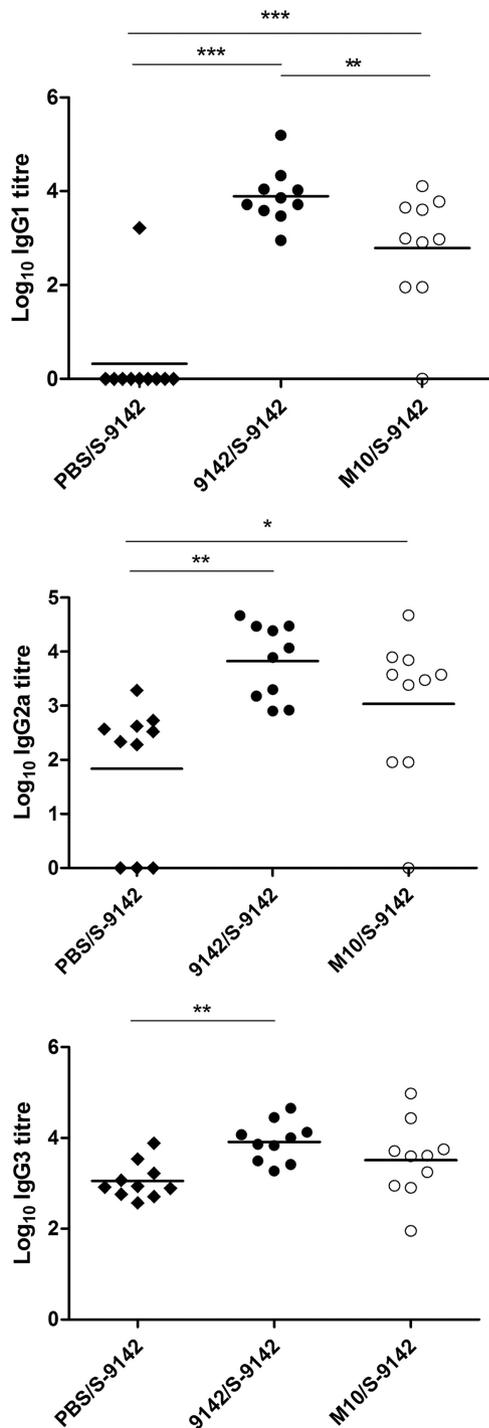
FIG 3 Serum *S. epidermidis*-specific IgG1, IgG2a, and IgG3 levels detected in *S. epidermidis*-immunized and -challenged mice given the immunization-and-challenge combination 9142/S-9142, M10/S-9142, or PBS/S-9142. IgG titers were determined in serum samples collected 4 days after i.v. infection with isopropanol-fixed S-9142 cells as the antigen to coat ELISA plates. Data are presented as $\log_{10}$ antibody titers, as indicated. Results correspond to pooled data of three independent experiments. Each dot represents an individual mouse. The horizontal line in each group represents the mean value. One-way ANOVA, $P < 0.05$, with Tukey's *post hoc* test: *, $P < 0.05$; **, $P < 0.01$; ***, $P < 0.001$.

plemental material, no significant differences were found among the different mouse groups in the proportions of splenic Foxp3-expressing $CD4^+$ $CD25^+$ or $CD4^+$ $CD25^-$ T cells or in Foxp3 expression levels in those populations. This indicates that PNAG did not induce T-cell differentiation into a Treg phenotype. However, splenic $CD4^+$ $CD25^+$ T cells sorted from 9142-immunized mice, and mostly containing $Foxp3^+$ cells (see Fig. S7), displayed a greater capacity to suppress anti-CD3 MAb-induced proliferation of $CD4^+$ $CD25^-$ responders than did counterparts obtained from control or M10-immune mice (Fig. 6). IL-10 was previously implicated in the suppressive function and stability of Tregs (28). Therefore, we investigated whether the higher suppressive activity of Tregs promoted by PNAG could be observed in $Il10^{-/-}$ mice. Notably, an inoculum of 2×10^8 *S. epidermidis* 9142 injected i.v., as used in WT mice, resulted in 100% mortality in $Il10^{-/-}$ mice. Thus, in subsequent studies, a 10-fold smaller dose was used for infections. $Il10^{-/-}$ mice immunized with either *S. epidermidis* strain developed liver pathology similar to that observed in WT mouse counterparts challenged with a greater bacterial load, with formation of granulomas (Fig. 7A and B). Compared to nonimmune controls, mice immunized with strain 9142 showed significant changes in cellular composition and an increase in the number of granulomas (Fig. 7A; see Fig. S5 in the supplemental material), as well as larger necrotic areas (Fig. 7C). As shown in Fig. 6, the greater suppressive activity displayed by Tregs obtained from the 9142-immune group was no longer observed in $Il10^{-/-}$ mice. As in the WT mice, the proportions of splenic $Foxp3^+$ $CD4^+$ $CD25^+$ and $CD4^+$ $CD25^-$ T cells were similar among the different mouse groups (see Fig. S8 in the supplemental material). These results implicate IL-10 in the generation of Tregs with higher suppressive activity detected in mice infected with 9142 bacteria. We next evaluated whether $Foxp3^+$ cells could be differently recruited into lesions observed in the livers of the different i.v. infected groups. As shown in Fig. S9 in the supplemental material, rare or no $Foxp3^+$ cells were detected in the lesions or surrounding tissue of all infected mice. These results show that although PNAG promoted the generation of Tregs with greater suppressive capacity, these cells were scarcely or not at all recruited into the hepatic lesions.

DISCUSSION

The PNAG homopolymer was initially shown to mediate intercellular adhesion of *S. epidermidis* biofilm cells (5) and to protect this bacterium from humoral and cellular immune mechanisms (16–18). Here we describe a proinflammatory effect of *S. epidermidis* PNAG. Mice inoculated i.p. with biofilm-grown *S. epidermidis* cells readily responded by recruiting neutrophils into the peritoneal cavity. The elevated levels of CXCL-1 and CXCL-2 detected in the peritoneal exudates of infected mice might have contributed to the neutrophil influx. *S. epidermidis*-induced production of CXCL-2 by human osteoblasts or murine epithelial cells and raised blood CXCL-1 levels have also been reported (29–31). Yet higher numbers of neutrophils were recruited into the peritoneal cavity in response to PNAG-positive strain 9142 than in response to PNAG-negative strain M10 in the very first hours following infection, thus explaining the faster bacterial clearance detected in the former infection. Nevertheless, at 24 h after infection, bacteria were already cleared by both mouse groups, in agreement with the low virulence usually attributed to *S. epidermidis* (1). Previous studies have shown that PNAG production may promote bacterial
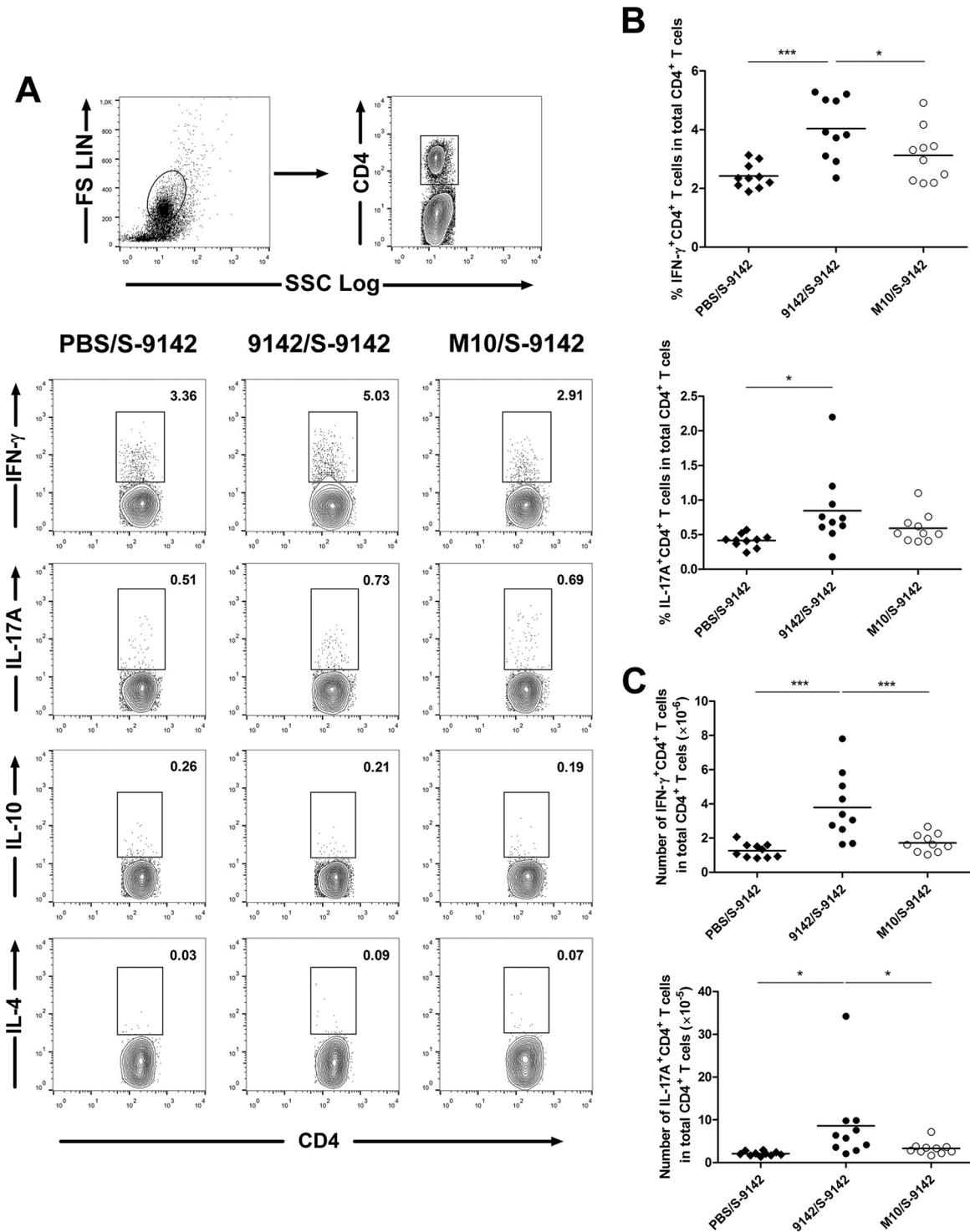
FIG 4 Proportions of splenic CD4$^+$ T cells producing IFN-γ and IL-17A. (A) Gating strategy and representative examples of flow cytometry analysis of CD4$^+$ T cells expressing IFN-γ, IL-17A, IL-10, and IL-4. (B, C) Proportions (B) and numbers (C) of IFN-γ^+ CD4$^+$ or IL-17A$^+$ CD4$^+$ T cells within total CD4$^+$ T cells detected 4 days after i.v. infection in the 9142/S-9142, M10/S-9142, and PBS/S-9142 mouse groups. Values within contour plots correspond to the frequencies of gated cells in the examples shown. Results correspond to pooled data of two independent experiments. Each dot corresponds to an individual mouse. The horizontal line in each group represents the mean value. One-way ANOVA, $P < 0.05$, with Tukey's *post hoc* test: *, $P < 0.05$; ***, $P < 0.001$. FS, forward scatter; SSC, side scatter.
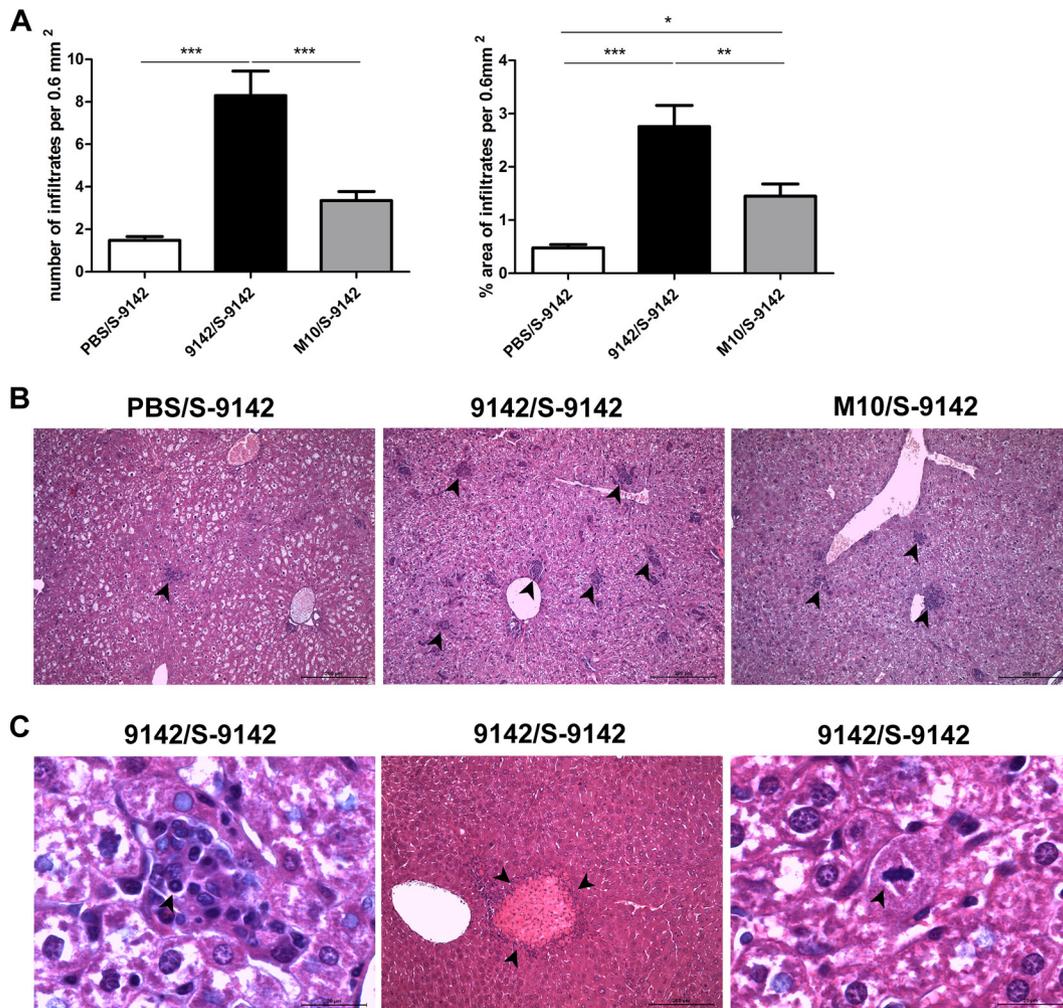
FIG 5 Analysis of liver histology in WT mice. (A) Quantitative analysis of the number of cellular infiltrates and the percentage of the area containing cellular infiltrates per 0.6 mm² in the livers of WT mice immunized and then challenged with *S. epidermidis* (9142/S-9142, M10/S-9142, and PBS/S-9142 groups) 4 days after i.v. infection. Bars represent mean values plus 1 standard deviation of six liver samples from each mouse group from which five micrographs from five different liver lobes were randomly taken at ×100 magnification. (B) Representative hematoxylin-eosin-stained examples of liver tissue from the mouse groups described above, as indicated above each image. (C) Representative micrographs of infiltrating neutrophils, necrotic areas, and hepatocyte mitosis in the left, middle, and right micrographs, respectively, observed in the *S. epidermidis*-immunized and then challenged 9142/S-9142 mouse group. The arrowheads in panel B indicate cell infiltrate clusters, and those in panel C indicate a neutrophil, a necrotic area, and a dividing hepatocyte, respectively. Bars, 200 or 20 μm, as indicated. One-way ANOVA, $P < 0.05$, with Tukey's *post hoc* test: *, $P < 0.05$; **, $P < 0.01$; ***, $P < 0.001$.

persistence in *S. epidermidis*-infected rodents (8, 9). This is in apparent contrast to the observation reported here of faster bacterial clearance of PNAG-producing bacteria. This discrepancy may be due to the device-associated biofilm infection model used in those studies instead of an i.p. established infection that does not promotes biofilm formation.

PBS-treated mice could control an i.v. infection with *S. epidermidis* originating from biofilms while developing only mild inflammatory pathology in the liver. Strikingly, priming with a small dose of biofilm-grown bacteria significantly exacerbated the hepatic inflammatory consequences of an i.v. challenge. Deleterious effects on the liver have also been observed in mice repeatedly challenged with *S. epidermidis* (32), indicating that chronic or repeated exposure to even at a small dose of this pathogen may significantly impact the usual harmless character of this bacterium. However, rare liver abscesses due to *S. epidermidis* infection have also been reported in human patients (33–36).

We observed here that *S. epidermidis*-infected mice responded by producing IFN-γ, in agreement with previous studies showing that murine dendritic cells challenged with 9142 biofilm cells secreted the IFN-γ-inducing cytokine IL-12 (37). Interestingly, although similar levels of IFN-γ were found in the serum of mice primed with either strain 9142 or M10, the former gave rise to higher frequencies of splenic IFN-γ-producing CD4+ T cells, indicating that PNAG on the bacterial cell promoted the differentiation of T cells producing this cytokine. IFN-γ may contribute to hepatocyte damage directly or indirectly through liver macrophage activation (38). Therefore, by favoring IFN-γ production, *S. epidermidis* PNAG could have contributed to the exacerbated liver inflammatory pathology observed in strain 9142-primed mice. The formation of granulomas observed in these mice further suggests the involvement of IFN-γ, as an important role for this cytokine in the organization of these inflammatory structures was previously reported (27). Production of IFN-γ, among other pro-
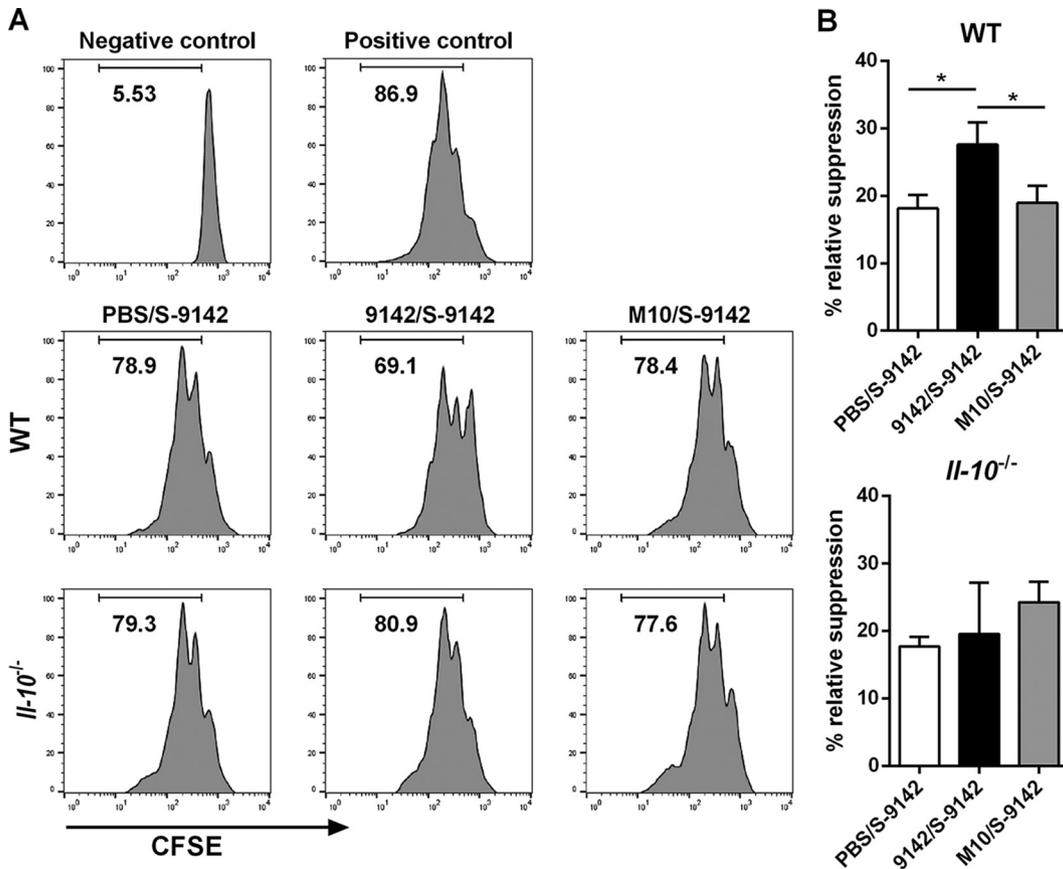
FIG 6 Flow cytometric evaluation of anti-CD3 MAb-induced proliferative response of 2.5×10^4 CFSE-labeled splenic naive CD4$^+$ CD25$^-$ T (responder) cells cultured for 72 h with 10^5 irradiated APC in the absence or presence of splenic CD4$^+$ CD25$^+$ T cells sorted from pooled splenic cells of three to five mice per group of 9142/S-9142, M10/S-9142, and PBS/S-9142 WT and $Il10^{-/-}$ mice, as indicated. The negative control corresponds to responder cells with no MAb added, and the positive control corresponds to responder cells cultured with MAb and without splenic CD4$^+$ CD25$^+$ T cells. (A) Histograms are representative examples out of three independent experiments and correspond to a 5:1 ratio of responder to CD4$^+$ CD25$^+$ T cells. Values are the percentages of cells that divided at least once. (B) Percentage of relative suppression exerted by CD4$^+$ CD25$^+$ T cells on the proliferative ability of responder cells. Bars correspond to mean values plus 1 standard deviation of data pooled from three independent experiments. The statistical significance of differences between mouse groups is indicated above the bars. One-way ANOVA, $P < 0.05$, with Tukey's *post hoc* test: *, $P < 0.05$.

inflammatory cytokines, has also been associated with clinical inflammation observed in *S. epidermidis*-induced experimental endophthalmitis (39). Nevertheless, antibody-mediated neutralization of IFN-γ indicates that this cytokine can actually be contributing to the control of the observed inflammatory pathology.

S. epidermidis 9142-primed mice also showed the highest frequencies of splenic IL-17A$^+$ CD4$^+$ T cells. IL-17 produced during bacterial infections has been associated with host protection rather than with hepatic damage (26, 40). However, studies investigating chronic bacterial infections (41, 42) or repeated immunization with mycobacterial antigens (43) have shown that this cytokine may contribute to immune-mediated tissue damage. Taking into account the recalcitrant nature of biofilm-originating infections, further studies will help elucidate whether IL-17A may affect host tissue integrity during these infections. IL-17-mediated pathology is usually associated with neutrophilic inflammation (43); however, this cytokine may also promote the formation of mononuclear cell granulomas (44). Therefore, a role for IL-17A in contributing to the formation of the hepatic lesions observed cannot be ruled out. It would be important to determine if there is a causal relationship between a granulomatous response and en-

hanced susceptibility to infection, as was suggested by some in zebrafish models of tuberculosis (45).

In apparent contrast to the proinflammatory effect of PNAG, Tregs from mice primed with PNAG-positive strain 9142 displayed greater suppressive activity than those primed with PNAG-negative strain M10 or control nonimmunized mice. The generation of Tregs with enhanced suppressive activity was also reported in studies related to other pathogens (22, 46) and may thus be a general phenomenon associated with infectious conditions. Nevertheless, a previous study showed that extracellular products of *S. epidermidis* promoted the suppressive activity of human Tregs (47), further indicating that this cell population may be involved in counterinflammatory mechanisms operating during infections with this bacterium. Tregs were recently shown to be crucial for establishing *S. epidermidis* skin commensalism (48). Taking our results into account, it will also be interesting to ascertain in future studies whether Tregs may contribute to the persistence of biofilm-related *S. epidermidis* infections (49). A limited role for Tregs in sustaining chronic *S. aureus* infection was previously reported (50). In the experimental model used here, the generation of Tregs with enhanced suppressive capacity depended on PNAG and IL-
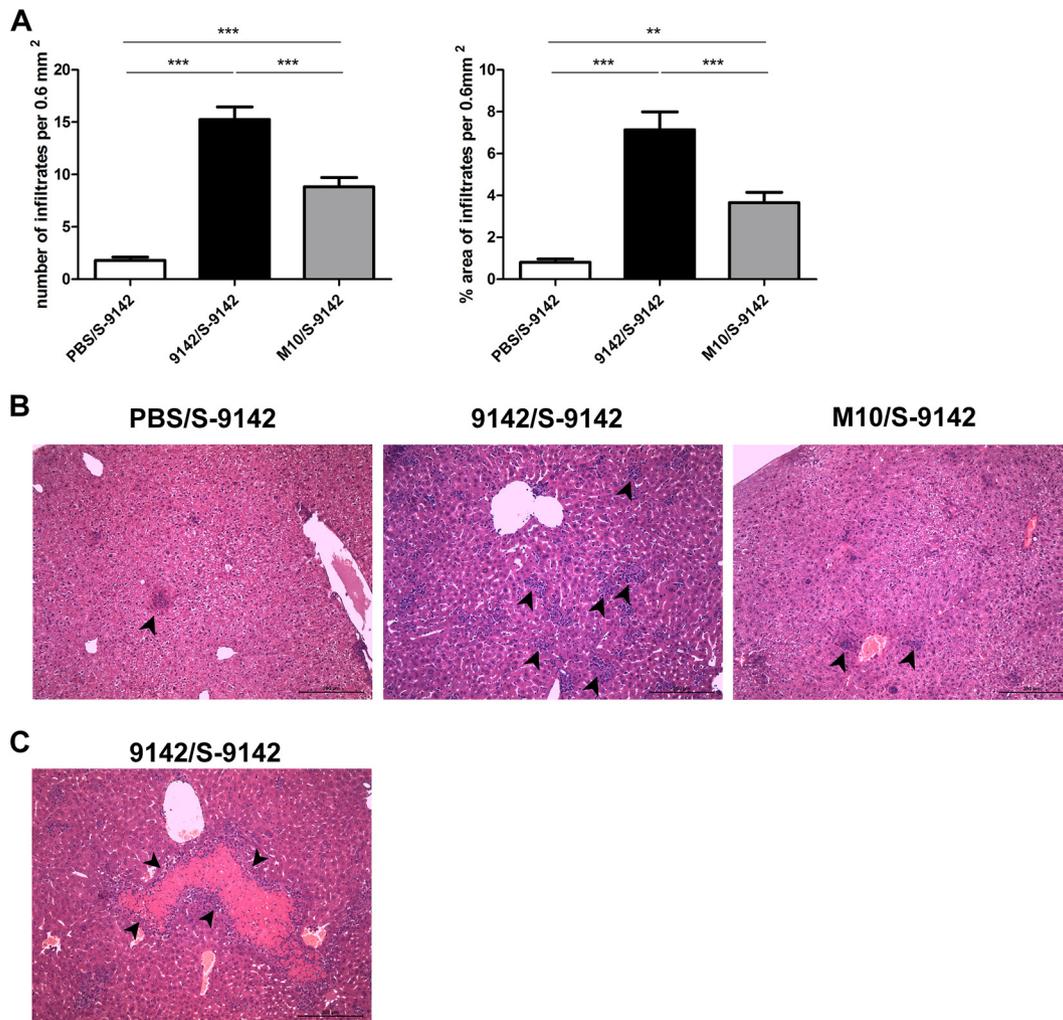
FIG 7 Analysis of liver histology in *Il10*$^{-/-}$ mice. (A) Quantitative analysis of the number of cellular infiltrates and the percentage of the area containing cellular infiltrates per 0.6 mm^2 observed 4 days after i.v. infection in the livers of *Il10*$^{-/-}$ mice from the *S. epidermidis*-immunized and then challenged 9142/S-9142, M10/S-9142, and PBS/S-9142 groups. Bars represent mean values plus 1 standard deviation of six liver samples from each *Il10*$^{-/-}$ mouse group from which five micrographs from five different liver lobes were randomly taken at ×100 magnification. (B) Representative hematoxylin-eosin-stained liver samples from the mouse groups described above, as indicated above the images. (C) Representative micrograph at ×400 magnification of a necrotic area observed in *S. epidermidis*-immunized and then challenged 9142/S-9142 *Il10*$^{-/-}$ mice. The arrowheads in panel B indicate cell infiltrate clusters, and those in panel C indicate a necrotic area. Bars, 200 μm. One-way ANOVA, $P < 0.05$, with Tukey's *post hoc* test: **, $P < 0.01$; ***, $P < 0.001$.

10. Production of IL-10 was favored by PNAG expression, as higher levels of this cytokine were found in the serum of mice challenged i.p. with PNAG-producing bacteria. Elevated IL-10 production in patients with staphylococcal bacteremia has been associated with an increased mortality rate, likely because of impaired immunity (51). However, as PNAG expression did not impair the clearance of 9142 bacteria while inducing IL-10 production, our results do not suggest a major role for this cytokine in the impairment of host immunity to *S. epidermidis*. The higher susceptibility to infection displayed by *Il10*$^{-/-}$ mice, which presented a more severe inflammatory pathology than WT counterparts, even when challenged with a 10-fold smaller dose of *S. epidermidis*, indicates that IL-10 may be more important in limiting excessive inflammation than in promoting bacterial persistence. Tregs are important in controlling excessive inflammation resulting from microbial infections (52). Therefore, it was somewhat surprising that mice of the 9142/S-9142 group simultaneously pre-sented highly suppressive Tregs and more marked liver tissue damage. A possible explanation may reside in the observed lack of Foxp3$^+$ cell recruitment into lesions.

S. epidermidis is a major cause of nosocomial bloodstream infections (53). Dispersal of biofilm-derived cells is thought to contribute significantly to the pathogenesis of systemic infections (54). Our results suggest that PNAG may contribute to pathogenesis by exacerbating the inflammatory response resulting from bacteremia. Previous reports have associated PNAG production with *S. epidermidis* virulence, mainly by assessing bacterial loads in target organs (9). Our results also implicate PNAG in the inflammatory pathology often associated with *S. epidermidis* infections (49). Moreover, by showing that this polysaccharide may exacerbate host tissue damage resulting from bacterial antigen priming, we unveiled another property of PNAG that may impact PNAG-targeted vaccination strategies. Together, by showing that PNAG may simultaneously contribute to pro- and counterinflammatory

mechanisms, the results presented here highlight the complex balance of the immune response elicited by *S. epidermidis* (14).

REFERENCES

1. **Otto M.** 2009. *Staphylococcus epidermidis*—the 'accidental' pathogen. Nat Rev Microbiol **7**:555–567. http://dx.doi.org/10.1038/nrmicro2182.

2. **Uçkay I, Pittet D, Vaudaux P, Sax H, Lew D, Waldvogel F.** 2009. Foreign body infections due to *Staphylococcus epidermidis*. Ann Med **41**:109–119. http://dx.doi.org/10.1080/07853890802337045.

3. **Götz F.** 2002. Staphylococcus and biofilms. Mol Microbiol **43**:1367–1378. http://dx.doi.org/10.1046/j.1365-2958.2002.02827.x.

4. **Mack D, Fischer W, Krokotsch A, Leopold K, Hartmann R, Egge H, Laufs R.** 1996. The intercellular adhesin involved in biofilm accumulation of *Staphylococcus epidermidis* is a linear beta-1,6-linked glucosaminoglycan: purification and structural analysis. J Bacteriol **178**:175–183.

5. **Mack D, Nedelmann M, Krokotsch A, Schwarzkopf A, Heesemann J, Laufs R.** 1994. Characterization of transposon mutants of biofilm-producing *Staphylococcus epidermidis* impaired in the accumulative phase of biofilm production: genetic identification of a hexosamine-containing polysaccharide intercellular adhesin. Infect Immun **62**:3244–3253.

6. **Heilmann C, Schweitzer O, Gerke C, Vanittanakom N, Mack D, Götz**

7. **Wang R, Khan BA, Cheung GY, Bach TH, Jameson-Lee M, Kong KF, Queck SY, Otto M.** 2011. *Staphylococcus epidermidis* surfactant peptides promote biofilm maturation and dissemination of biofilm-associated infection in mice. J Clin Invest **121**:238–248. http://dx.doi.org/10.1172/JCI42520.

8. **Rupp ME, Ulphani JS, Fey PD, Bartscht K, Mack D.** 1999. Characterization of the importance of polysaccharide intercellular adhesin/hemagglutinin of *Staphylococcus epidermidis* in the pathogenesis of biomaterial-based infection in a mouse foreign body infection model. Infect Immun **67**:2627–2632.

9. **Rupp ME, Ulphani JS, Fey PD, Mack D.** 1999. Characterization of *Staphylococcus epidermidis* polysaccharide intercellular adhesin/hemagglutinin in the pathogenesis of intravascular catheter-associated infection in a rat model. Infect Immun **67**:2656–2659.

10. **Begun J, Gaiani JM, Rohde H, Mack D, Calderwood SB, Ausubel FM, Sifri CD.** 2007. Staphylococcal biofilm exopolysaccharide protects against *Caenorhabditis elegans* immune defenses. PLoS Pathog **3**:e57. http://dx.doi.org/10.1371/journal.ppat.0030057.

11. **Fluckiger U, Ulrich M, Steinhuber A, Doring G, Mack D, Landmann R, Goerke C, Wolz C.** 2005. Biofilm formation, *icaADBC* transcription, and polysaccharide intercellular adhesin synthesis by staphylococci in a device-related infection model. Infect Immun **73**:1811–1819. http://dx.doi.org/10.1128/IAI.73.3.1811-1819.2005.

12. **Li H, Xu L, Wang J, Wen Y, Vuong C, Otto M, Gao Q.** 2005. Conversion of *Staphylococcus epidermidis* strains from commensal to invasive by expression of the *ica* locus encoding production of biofilm exopolysaccharide. Infect Immun **73**:3188–3191. http://dx.doi.org/10.1128/IAI.73.5.3188-3191.2005.

13. **Diemond-Hernández B, Solorzano-Santos F, Leanos-Miranda B, Peregrino-Bejarano L, Miranda-Novales G.** 2010. Production of icaADBC-encoded polysaccharide intercellular adhesin and therapeutic failure in pediatric patients with staphylococcal device-related infections. BMC Infect Dis **10**:68. http://dx.doi.org/10.1186/1471-2334-10-68.

14. **Fredheim EG, Granslo HN, Flaegstad T, Figenschau Y, Rohde H, Sadovskaya I, Mollnes TE, Klingenberg C.** 2011. *Staphylococcus epidermidis* polysaccharide intercellular adhesin activates complement. FEMS Immunol Med Microbiol **63**:269–280. http://dx.doi.org/10.1111/j.1574-695X.2011.00854.x.

15. **Stevens NT, Sadovskaya I, Jabbouri S, Sattar T, O'Gara JP, Humphreys H, Greene CM.** 2009. *Staphylococcus epidermidis* polysaccharide intercellular adhesin induces IL-8 expression in human astrocytes via a mechanism involving TLR2. Cell Microbiol **11**:421–432. http://dx.doi.org/10.1111/j.1462-5822.2008.01264.x.

16. **Kristian SA, Birkenstock TA, Sauder U, Mack D, Götz F, Landmann R.** 2008. Biofilm formation induces C3a release and protects *Staphylococcus epidermidis* from IgG and complement deposition and from neutrophil-dependent killing. J Infect Dis **197**:1028–1035. http://dx.doi.org/10.1086/528992.

17. **Vuong C, Voyich JM, Fischer ER, Braughton KR, Whitney AR, DeLeo FR, Otto M.** 2004. Polysaccharide intercellular adhesin (PIA) protects *Staphylococcus epidermidis* against major components of the human innate immune system. Cell Microbiol **6**:269–275. http://dx.doi.org/10.1046/j.1462-5822.2004.00367.x.

18. **Cerca N, Jefferson KK, Oliveira R, Pier GB, Azeredo J.** 2006. Comparative antibody-mediated phagocytosis of *Staphylococcus epidermidis* cells grown in a biofilm or in the planktonic state. Infect Immun **74**:4849–4855. http://dx.doi.org/10.1128/IAI.00230-06.

19. **Mack D, Siemssen N, Laufs R.** 1992. Parallel induction by glucose of adherence and a polysaccharide antigen specific for plastic-adherent *Staphylococcus epidermidis*: evidence for functional relation to intercellular adhesion. Infect Immun **60**:2048–2057.

20. **Cerca F, Trigo G, Correia A, Cerca N, Azeredo J, Vilanova M.** 2011. SYBR green as a fluorescent probe to evaluate the biofilm physiological state of *Staphylococcus epidermidis*, using flow cytometry. Can J Microbiol **57**:850–856. http://dx.doi.org/10.1139/w11-078.

21. **França A, Carvalhais V, Vilanova M, Pier G, Cerca N.** 2016. Characterization of an in vitro fed-batch model to obtain cells released from *S. epidermidis* biofilms. AMB Express **6**:23. http://dx.doi.org/10.1186/s13568-016-0197-9.

22. **Correia A, Ferreirinha P, Costa AA, Dias J, Melo J, Costa R, Ribeiro A,**

Faustino A, Teixeira L, Rocha A, Vilanova M. 2013. Mucosal and systemic T cell response in mice intragastrically infected with *Neospora caninum* tachyzoites. Vet Res **44:**69. http://dx.doi.org/10.1186/1297-9716-44-69.

23. Teixeira L, Moreira J, Melo J, Bezerra F, Marques RM, Ferreirinha P, Correia A, Monteiro MP, Ferreira PG, Vilanova M. 2015. Immune response in the adipose tissue of lean mice infected with the protozoan parasite *Neospora caninum*. Immunology **145:**242–257. http://dx.doi.org/10.1111/imm.12440.

24. Daley JM, Thomay AA, Connolly MD, Reichner JS, Albina JE. 2008. Use of Ly6G-specific monoclonal antibody to deplete neutrophils in mice. J Leukoc Biol **83:**64–70. http://dx.doi.org/10.1189/jlb.0407247.

25. Boles BR, Horswill AR. 2011. Staphylococcal biofilm disassembly. Trends Microbiol **19:**449–455. http://dx.doi.org/10.1016/j.tim.2011.06.004.

26. Chung HM, Cartwright MM, Bortz DM, Jackson TL, Younger JG. 2008. Dynamical system analysis of *Staphylococcus epidermidis* bloodstream infection. Shock **30:**518–526. http://dx.doi.org/10.1097/SHK.0b013e31816a0b77.

27. Appelberg R, Moreira D, Barreira-Silva P, Borges M, Silva L, Dinis-Oliveira RJ, Resende M, Correia-Neves M, Jordan MB, Ferreira NC, Abrunhosa AJ, Silvestre R. 2015. The Warburg effect in mycobacterial granulomas is dependent on the recruitment and activation of macrophages by interferon-γ. Immunology **145:**498–507. http://dx.doi.org/10.1111/imm.12464.

28. Verhagen J, Wegner A, Wraith DC. 2015. Extra-thymically induced T regulatory cell subsets: the optimal target for antigen-specific immunotherapy. Immunology **145:**171–181. http://dx.doi.org/10.1111/imm.12458.

29. Dapunt U, Maurer S, Giese T, Gaida MM, Hansch GM. 2014. The macrophage inflammatory proteins MIP1α (CCL3) and MIP2α (CXCL2) in implant-associated osteomyelitis: linking inflammation to bone degradation. Mediators Inflamm **2014:**728619. http://dx.doi.org/10.1155/2014/728619.

30. Val S, Mubeen H, Tomney A, Chen S, Preciado D. 2015. Impact of *Staphylococcus epidermidis* lysates on middle ear epithelial proinflammatory and mucogenic response. J Investig Med **63:**258–266. http://dx.doi.org/10.1097/JIM.0000000000000127.

31. Schroder K, Hertzog PJ, Ravasi T, Hume DA. 2004. Interferon-gamma: an overview of signals, mechanisms and functions. J Leukoc Biol **75:**163–189. http://dx.doi.org/10.1189/jlb.0603252.

32. Akinkunmi EO, Adeyemi OI, Igbeneghu OA, Olaniyan EO, Omonisi AE, Lamikanra A. 2014. The pathogenicity of *Staphylococcus epidermidis* on the intestinal organs of rats and mice: an experimental investigation. BMC Gastroenterol **14:**126. http://dx.doi.org/10.1186/1471-230X-14-126.

33. Miller TE. 1974. *Staphylococcus epidermidis* as a cause of liver abscess: case report. N Z Med J **79:**692–693.

34. Pagano L, Larocca LM, Marra R, Pizzigallo E, Leone G. 1992. A leukemic patient with hepatosplenic abscesses due to coagulase-negative staphylococci. Clin Infect Dis **14:**364–365. http://dx.doi.org/10.1093/clinids/14.1.364.

35. Mechaber AJ, Tuazon CU. 1997. Hepatic abscess: rare complication of ventriculoperitoneal shunts. Clin Infect Dis **25:**1244–1245. http://dx.doi.org/10.1086/516957.

36. Tsukuda K, Furutani S, Nakahara S, Tada A, Watanabe K, Takagi S, Ikeda E, Hirai R, Tsuji H. 2008. Abscess formation of the round ligament of the liver: report of a case. Acta Med Okayama **62:**411–413.

37. Cerca F, França A, Perez-Cabezas B, Carvalhais V, Ribeiro A, Azeredo J, Pier G, Cerca N, Vilanova M. 2014. Dormant bacteria within *Staphylococcus epidermidis* biofilms have low inflammatory properties and maintain tolerance to vancomycin and penicillin after entering planktonic growth. J Med Microbiol **63:**1274–1283. http://dx.doi.org/10.1099/jmm.0.073163-0.

38. Horras CJ, Lamb CL, Mitchell KA. 2011. Regulation of hepatocyte fate by interferon-gamma. Cytokine Growth Factor Rev **22:**35–43. http://dx.doi.org/10.1016/j.cytogfr.2011.01.001.

39. Petropoulos IK, Vantzou CV, Lamari FN, Karamanos NK, Anastassiou ED, Pharmakakis NM. 2006. Expression of TNF-alpha, IL-1beta, and IFN-gamma in *Staphylococcus epidermidis* slime-positive experimental endophthalmitis is closely related to clinical inflammatory scores. Graefes Arch Clin Exp Ophthalmol **244:**1322–1328. http://dx.doi.org/10.1007/s00417-006-0261-2.

40. Hammerich L, Heymann F, Tacke F. 2011. Role of IL-17 and Th17 cells in liver diseases. Clin Dev Immunol **2011:**345803. http://dx.doi.org/10.1155/2011/345803.

41. Fedele G, Nasso M, Spensieri F, Palazzo R, Frasca L, Watanabe M, Ausiello CM. 2008. Lipopolysaccharides from *Bordetella pertussis* and *Bordetella parapertussis* differently modulate human dendritic cell functions resulting in divergent prevalence of Th17-polarized responses. J Immunol **181:**208–216. http://dx.doi.org/10.4049/jimmunol.181.1.208.

42. Luzza F, Parrello T, Monteleone G, Sebkova L, Romano M, Zarrilli R, Imeneo M, Pallone F. 2000. Up-regulation of IL-17 is associated with bioactive IL-8 expression in *Helicobacter pylori*-infected human gastric mucosa. J Immunol **165:**5332–5337. http://dx.doi.org/10.4049/jimmunol.165.9.5332.

43. Cruz A, Fraga AG, Fountain JJ, Rangel-Moreno J, Torrado E, Saraiva M, Pereira DR, Randall TD, Pedrosa J, Cooper AM, Castro AG. 2010. Pathological role of interleukin 17 in mice subjected to repeated BCG vaccination after infection with *Mycobacterium tuberculosis*. J Exp Med **207:**1609–1616. http://dx.doi.org/10.1084/jem.20100265.

44. Hamada S, Umemura M, Shiono T, Tanaka K, Yahagi A, Begum MD, Oshiro K, Okamoto Y, Watanabe H, Kawakami K, Roark C, Born WK, O'Brien R, Ikuta K, Ishikawa H, Nakae S, Iwakura Y, Ohta T, Matsuzaki G. 2008. IL-17A produced by gammadelta T cells plays a critical role in innate immunity against *Listeria monocytogenes* infection in the liver. J Immunol **181:**3456–3463. http://dx.doi.org/10.4049/jimmunol.181.5.3456.

45. Ramakrishnan L. 2013. Looking within the zebrafish to understand the tuberculous granuloma. Adv Exp Med Biol **783:**251–266. http://dx.doi.org/10.1007/978-1-4614-6111-1_13.

46. Johanns TM, Ertelt JM, Rowe JH, Way SS. 2010. Regulatory T cell suppressive potency dictates the balance between bacterial proliferation and clearance during persistent Salmonella infection. PLoS Pathog **6:**e1001043. http://dx.doi.org/10.1371/journal.ppat.1001043.

47. Laborel-Préneron E, Bianchi P, Boralevi F, Lehours P, Fraysse F, Morice-Picard F, Sugai M, Sato'o Y, Badiou C, Lina G, Schmitt AM, Redoules D, Casas C, Davrinche C. 2015. Effects of the *Staphylococcus aureus* and *Staphylococcus epidermidis* secretomes isolated from the skin microbiota of atopic children on CD4$^+$ T cell activation. PLoS One **10:**e0141067. http://dx.doi.org/10.1371/journal.pone.0141067.

48. Scharschmidt TC, Vasquez KS, Truong HA, Gearty SV, Pauli ML, Nosbaum A, Gratz IK, Otto M, Moon JJ, Liese J, Abbas AK, Fischbach MA, Rosenblum MD. 2015. A wave of regulatory T cells into neonatal skin mediates tolerance to commensal microbes. Immunity **43:**1011–1021. http://dx.doi.org/10.1016/j.immuni.2015.10.016.

49. Römling U, Balsalobre C. 2012. Biofilm infections, their resilience to therapy and innovative treatment strategies. J Intern Med **272:**541–561. http://dx.doi.org/10.1111/joim.12004.

50. Tebartz C, Horst SA, Sparwasser T, Huehn J, Beineke A, Peters G, Medina E. 2015. A major role for myeloid-derived suppressor cells and a minor role for regulatory T cells in immunosuppression during *Staphylococcus aureus* infection. J Immunol **194:**1100–1111. http://dx.doi.org/10.4049/jimmunol.1400196.

51. Peres AG, Madrenas J. 2013. The broad landscape of immune interactions with *Staphylococcus aureus*: from commensalism to lethal infections. Burns **39:**380–388. http://dx.doi.org/10.1016/j.burns.2012.12.008.

52. Belkaid Y, Tarbell K. 2009. Regulatory T cells in the control of host-microorganism interactions. Annu Rev Immunol **27:**551–589. http://dx.doi.org/10.1146/annurev.immunol.021908.132723.

53. Hidron AI, Edwards JR, Patel J, Horan TC, Sievert DM, Pollock DA, Fridkin SK. 2008. NHSN annual update: antimicrobial-resistant pathogens associated with healthcare-associated infections: annual summary of data reported to the National Healthcare Safety Network at the Centers for Disease Control and Prevention, 2006-2007. Infect Control Hosp Epidemiol **29:**996–1011. http://dx.doi.org/10.1086/591861.

54. Kaplan JB. 2010. Biofilm dispersal: mechanisms, clinical implications, and potential therapeutic uses. J Dent Res **89:**205–218. http://dx.doi.org/10.1177/0022034509359403.